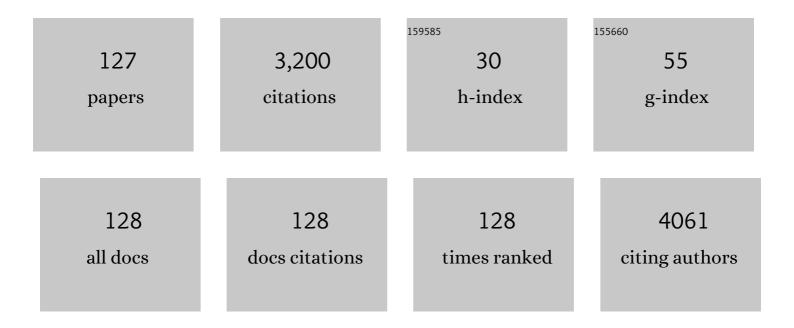
## **Pauls Stradins**

List of Publications by Year in descending order

Source: https://exaly.com/author-pdf/3867267/publications.pdf Version: 2024-02-01



#	Article	IF	CITATIONS
1	Accelerated reliability tests of n+ and p+ poly-Si passivated contacts. Solar Energy Materials and Solar Cells, 2022, 236, 111469.	6.2	3
2	Measurement of poly-Si film thickness on textured surfaces by X-ray diffraction in poly-Si/SiO passivating contacts for monocrystalline Si solar cells. Solar Energy Materials and Solar Cells, 2022, 236, 111510.	6.2	9
3	Self-Aligned Selective Area Front Contacts on <i>Poly</i> -Si/SiO <i> <sub>x</sub> </i> Passivating Contact <i>c</i> -Si Solar Cells. IEEE Journal of Photovoltaics, 2022, 12, 678-689.	2.5	10
4	Atomic structure of light-induced efficiency-degrading defects in boron-doped Czochralski silicon solar cells. Energy and Environmental Science, 2021, 14, 5416-5422.	30.8	6
5	Outdoor performance of a tandem InGaP/Si photovoltaic luminescent solar concentrator. Solar Energy Materials and Solar Cells, 2021, 223, 110945.	6.2	13
6	Chemical Passivation of Crystalline Si by Al <sub>2</sub> O <sub>3</sub> Deposited Using Atomic Layer Deposition: Implications for Solar Cells. ACS Applied Nano Materials, 2021, 4, 6629-6636.	5.0	6
7	Effective Dielectric Passivation Scheme in Area-Selective Front/Back Poly-Si/SiOx Passivating Contact Solar Cells. , 2021, , .		0
8	Electron Paramagentic Resonance Investigation of Mechanism of Light- and Elevated-Temperature-Induced Degradation in Ga-doped Cz Si. , 2021, , .		0
9	Fabrication of Poly-Si on Locally Etched SiOx as Passivating Contacts for c-Si Solar Cells. , 2021, , .		0
10	Trap-Assisted Dopant Compensation Prevents Shunting in poly-Si Passivating Interdigitated Back Contact Silicon Solar Cells. , 2021, , .		0
11	Trap-Assisted Dopant Compensation Prevents Shunting in Poly-Si Passivating Interdigitated Back Contact Silicon Solar Cells. ACS Applied Energy Materials, 2021, 4, 10774-10782.	5.1	8
12	Three-terminal III–V/Si tandem solar cells enabled by a transparent conductive adhesive. Sustainable Energy and Fuels, 2020, 4, 549-558.	4.9	46
13	Probing the Evolution of Surface Chemistry at the Silicon–Electrolyte Interphase via In Situ Surface-Enhanced Raman Spectroscopy. Journal of Physical Chemistry Letters, 2020, 11, 286-291.	4.6	23
14	Effect of Water Concentration in LiPF <sub>6</sub> -Based Electrolytes on the Formation, Evolution, and Properties of the Solid Electrolyte Interphase on Si Anodes. ACS Applied Materials & Interfaces, 2020, 12, 49563-49573.	8.0	27
15	Effect of Surface Texture on Pinhole Formation in SiO <i><sub>x</sub></i> -Based Passivated Contacts for High-Performance Silicon Solar Cells. ACS Applied Materials & Interfaces, 2020, 12, 55737-55745.	8.0	18
16	Influence of Tabula Rasa on Process- and Light-Induced Degradation of Solar Cells Fabricated From Czochralski Silicon. IEEE Journal of Photovoltaics, 2020, 10, 1557-1565.	2.5	4
17	Isolating p- and n-Doped Fingers With Intrinsic Poly-Si in Passivated Interdigitated Back Contact Silicon Solar Cells. IEEE Journal of Photovoltaics, 2020, 10, 1574-1581.	2.5	12
18	Reactive ion etched, self-aligned, selective area poly-Si/SiO2 passivated contacts. Solar Energy Materials and Solar Cells, 2020, 217, 110621.	6.2	18

#	Article	IF	CITATIONS
19	Enhanced Interfacial Stability of Si Anodes for Li-Ion Batteries via Surface SiO <sub>2</sub> Coating. ACS Applied Energy Materials, 2020, 3, 8842-8849.	5.1	38
20	Surface SiO <sub>2</sub> Thickness Controls Uniform-to-Localized Transition in Lithiation of Silicon Anodes for Lithium-Ion Batteries. ACS Applied Materials & Interfaces, 2020, 12, 27017-27028.	8.0	37
21	On the hydrogenation of Poly-Si passivating contacts by Al2O3 and SiN thin films. Solar Energy Materials and Solar Cells, 2020, 215, 110592.	6.2	53
22	Spectroscopic Investigation of Light-Induced Degradation Paramagnetic Defect in Czochralski Silicon. , 2020, , .		1
23	Understanding the origin of Tabula Rasa process-induced defects in CZ n-type c-Si. , 2020, , .		0
24	Submicron Thickness Characterization of poly-Si thin films on Textured Surfaces by X-ray Diffraction for Minimizing Parasitic Absorption in Poly-Si/SiO2 Passivating Contact Cells. , 2020, , .		0
25	Pinhole formation in poly-Si/SiOx passivating contacts on Si(111)-oriented textures. , 2020, , .		Ο
26	Effect of Dopant Compensation on the Conductivity of the Intrinsic poly-Si Isolation Region in Passivated IBC Silicon Solar Cells. , 2020, , .		1
27	<i>Tabula Rasa</i> for <i>n</i> z siliconâ€based photovoltaics. Progress in Photovoltaics: Research and Applications, 2019, 27, 136-143.	8.1	12
28	Effect of Crystallographic Orientation and Nanoscale Surface Morphology on Poly-Si/SiO <sub><i>x</i></sub> Contacts for Silicon Solar Cells. ACS Applied Materials & Interfaces, 2019, 11, 42021-42031.	8.0	29
29	Critical interface: Poly-silicon to tunneling SiO2 for passivated contact performance. AIP Conference Proceedings, 2019, , .	0.4	2
30	Modifications of Textured Silicon Surface Morphology and Its Effect on Poly-Si/SiO <i> <sub>x</sub> </i> Contact Passivation for Silicon Solar Cells. IEEE Journal of Photovoltaics, 2019, 9, 1513-1521.	2.5	13
31	Backâ€contacted bottom cells with three terminals: Maximizing power extraction from currentâ€mismatched tandem cells. Progress in Photovoltaics: Research and Applications, 2019, 27, 410-423.	8.1	31
32	Understanding the charge transport mechanisms through ultrathin SiO <i>x</i> layers in passivated contacts for high-efficiency silicon solar cells. Applied Physics Letters, 2019, 114, .	3.3	41
33	Luminescent Solar Concentrator Tandem-on-Silicon with above 700mV Passivated Contact Silicon Bottom Cell. , 2019, , .		Ο
34	Enhancing Photocarrier Bulk Lifetime with Defect Engineering of Polycrystalline Passivated-Contact n-Cz Photovoltaic Devices. , 2019, , .		0
35	Self-Aligned, Selective Area Poly-Si/SiO <sub>2</sub> Passivated Contacts for Enhanced Photocurrent in Front/Back Solar Cells. , 2019, , .		1
36	Mitigating Process Induced Degradation in p- and n-Czochralski Silicon Wafers with Tabula Rasa. , 2019, , .		0

#	Article	IF	CITATIONS
37	Nonuniform Charge Collection in SiO <sub>x</sub> -Based Passivated-Contact Silicon Solar Cells. , 2019, , .		1
38	Understanding and Mitigating the Contamination of Intrinsic poly-Si Gaps in Passivated IBC Solar Cells. , 2019, , .		0
39	III-V/Si Tandem Cells Utilizing Interdigitated Back Contact Si Cells and Varying Terminal Configurations. , 2019, , .		2
40	Transparent Conductive Adhesives for Tandem Solar Cells Using Polymer–Particle Composites. ACS Applied Materials & Interfaces, 2018, 10, 8086-8091.	8.0	25
41	Maximizing tandem solar cell power extraction using a three-terminal design. Sustainable Energy and Fuels, 2018, 2, 1141-1147.	4.9	67
42	Growth of amorphous and epitaxial ZnSiP <sub>2</sub> –Si alloys on Si. Journal of Materials Chemistry C, 2018, 6, 2696-2703.	5.5	18
43	Charge carrier transport mechanisms of passivating contacts studied by temperature-dependent J-V measurements. Solar Energy Materials and Solar Cells, 2018, 178, 15-19.	6.2	78
44	Tunneling or Pinholes: Understanding the Transport Mechanisms in SiO <inf>x</inf> Based Passivated Contacts for High-Efficiency Silicon Solar Cells. , 2018, , .		7
45	Operating principles of three-terminal solar cells. , 2018, , .		4
46	Equivalent Performance in Three-Terminal and Four-Terminal Tandem Solar Cells. IEEE Journal of Photovoltaics, 2018, 8, 1584-1589.	2.5	31
47	Hydrogen passivation of poly-Si/SiOx contacts for Si solar cells using Al2O3 studied with deuterium. Applied Physics Letters, 2018, 112, .	3.3	80
48	Yield analysis and comparison of GaInP/Si and GaInP/GaAs multi-terminal tandem solar cells. AIP Conference Proceedings, 2018, , .	0.4	2
49	Effect of silicon oxide thickness on polysilicon based passivated contacts for high-efficiency crystalline silicon solar cells. Solar Energy Materials and Solar Cells, 2018, 185, 270-276.	6.2	60
50	Effect of the SiO2 interlayer properties with solid-source hydrogenation on passivated contact performance and surface passivation. Energy Procedia, 2017, 124, 295-301.	1.8	24
51	Nonisovalent Si-III-V and Si-II-VI alloys: Covalent, ionic, and mixed phases. Physical Review B, 2017, 96, .	3.2	2
52	A Novel Method to Investigate Stoichiometry and Performance of Buried Passivated Contacts Utilizing Time-of-Flight SIMS. , 2017, , .		0
53	III-V/Si tandem cell to module interconnection - comparison between different operation modes. , 2017, , $\cdot$		1
54	An Isotope Study of Hydrogen Passivation of poly-Si/SiOx Passivated Contacts for Si Solar Cells. , 2017, , .		0

#	Article	IF	CITATIONS
55	Dopant Patterning by PECVD and Mechanical Masking for Passivated Tunneling Contact IBC Cell Architectures. , 2017, , .		0
56	Self Aligned Aluminum Selective Emitter for n-type Si Cells. , 2017, , .		0
57	the Iimplied Voc of Passivated Contacts for c-Si Based Solar Cells. , 2017, , .		0
58	Tabula Rasa: Oxygen precipitate dissolution though rapid high temperature processing in silicon. , 2017, , .		0
59	Modeling three-terminal III- V ISi tandem solar cells. , 2017, , .		1
60	Transparent Conductive Adhesives for Tandem Solar Cells. , 2017, , .		5
61	Air Passivation of Chalcogen Vacancies in Twoâ€Dimensional Semiconductors. Angewandte Chemie, 2016, 128, 977-980.	2.0	15
62	Air Passivation of Chalcogen Vacancies in Twoâ€Đimensional Semiconductors. Angewandte Chemie - International Edition, 2016, 55, 965-968.	13.8	80
63	Atomic scale understanding of poly-Si/SiO <inf>2</inf> /c-Si passivated contacts: Passivation degradation due to metallization. , 2016, , .		3
64	Selective area growth of GaAs on Si patterned using nanoimprint lithography. , 2016, , .		6
65	Plasma immersion ion implantation for interdigitated back passivated contact (IBPC) solar cells. , 2016, , .		1
66	Energy conversion properties of ZnSiP <inf>2</inf> , a lattice-matched material for silicon-based tandem photovoltaics. , 2016, , .		2
67	Study of nickel silicide as a copper diffusion barrier in monocrystalline silicon solar cells. , 2016, , .		4
68	Bandgap and carrier transport engineering of quantum confined mixed phase nanocrystalline/amorphous silicon. , 2016, , .		1
69	Polycrystalline silicon passivated tunneling contacts for high efficiency silicon solar cells. Journal of Materials Research, 2016, 31, 671-681.	2.6	133
70	Realization of GalnP/Si Dual-Junction Solar Cells With 29.8% 1-Sun Efficiency. IEEE Journal of Photovoltaics, 2016, 6, 1012-1019.	2.5	114
71	Low-cost plasma immersion ion implantation doping for Interdigitated back passivated contact (IBPC) solar cells. Solar Energy Materials and Solar Cells, 2016, 158, 68-76.	6.2	37
72	Van der Waals metal-semiconductor junction: Weak Fermi level pinning enables effective tuning of Schottky barrier. Science Advances, 2016, 2, e1600069.	10.3	446

#	Article	IF	CITATIONS
73	Quasi-Direct Optical Transitions in Silicon Nanocrystals with Intensity Exceeding the Bulk. Nano Letters, 2016, 16, 1583-1589.	9.1	62
74	Interdigitated Back Passivated Contact (IBPC) Solar Cells Formed by Ion Implantation. IEEE Journal of Photovoltaics, 2016, 6, 41-47.	2.5	36
75	Growth of antiphase-domain-free GaP on Si substrates by metalorganic chemical vapor deposition using an <i>in situ</i> AsH3 surface preparation. Applied Physics Letters, 2015, 107, .	3.3	51
76	Tunnel oxide passivated contacts formed by ion implantation for applications in silicon solar cells. Journal of Applied Physics, 2015, 118, .	2.5	65
77	Ion implanted passivated contacts for interdigitated back contacted solar cells. , 2015, , .		3
78	Indium zinc oxide mediated wafer bonding for IIIâ $\in$ "V/Si tandem solar cells. , 2015, , .		8
79	Progress Towards a 30% Efficient GaInP/Si Tandem Solar Cell. Energy Procedia, 2015, 77, 464-469.	1.8	87
80	Comparison of thin epitaxial film silicon photovoltaics fabricated on monocrystalline and polycrystalline seed layers on glass. Progress in Photovoltaics: Research and Applications, 2015, 23, 909-917.	8.1	9
81	Bulk defect generation during B-diffusion and oxidation of CZ wafers: Mechanism for degrading solar cell performance. , 2014, , .		3
82	Free standing silica thin films with highly ordered perpendicular nanopores. RSC Advances, 2014, 4, 7627-7633.	3.6	15
83	Study of the passivation mechanism of c-Si by Al <inf>2</inf> O <inf>3</inf> using in situ infrared spectroscopy. , 2014, , .		1
84	Dielectric stack passivation on boron- and phosphorus-diffused surfaces and 20% efficient PERT cell on n-CZ silicon substrate. , 2014, , .		0
85	Reformulation of solar cell physics to facilitate experimental separation of recombination pathways. Applied Physics Letters, 2013, 103, .	3.3	78
86	Device Physics of Heteroepitaxial Film c-Si Heterojunction Solar Cells. IEEE Journal of Photovoltaics, 2013, 3, 230-235.	2.5	8
87	600 mV epitaxial crystal silicon solar cells grown on seeded glass. , 2013, , .		4
88	Improved 750 °C epitaxial crystal silicon solar cells through impurity reduction. , 2013, , .		1
89	New analysis of suns-V <inf>oc</inf> and V <inf>oc</inf> (T): A simple method to quantify recombination channels in solar cells. , 2013, , .		0
90	Device physics of heteroepitaxial film c-Si heterojunction solar cells. , 2013, , .		0

#	Article	IF	CITATIONS
91	Dislocation-limited open circuit voltage in film crystal silicon solar cells. Applied Physics Letters, 2012, 101, 123510.	3.3	6
92	Device physics of heteroepitaxial film c-Si heterojunction solar cells. , 2012, , .		1
93	Synthesis and characterization of PECVD-grown, silane-terminated silicon quantum dots. , 2012, , .		2
94	Strained Interface Defects in Silicon Nanocrystals. Advanced Functional Materials, 2012, 22, 3223-3232.	14.9	63
95	In Situ Gas-Phase Hydrosilylation of Plasma-Synthesized Silicon Nanocrystals. ACS Applied Materials & Interfaces, 2011, 3, 3033-3041.	8.0	50
96	Matrix-embedded silicon quantum dots for photovoltaic applications: a theoretical study of critical factors. Energy and Environmental Science, 2011, 4, 2546.	30.8	72
97	Tin-Catalyzed Plasma-Assisted Growth of Silicon Nanowires. Journal of Physical Chemistry C, 2011, 115, 3833-3839.	3.1	54
98	Anneal treatment to reduce the creation rate of light-induced metastable defects in device-quality hydrogenated amorphous silicon. Applied Physics Letters, 2011, 98, 201908.	3.3	17
99	Light trapping by a dielectric nanoparticle back reflector in film silicon solar cells. Applied Physics Letters, 2011, 99, 064101.	3.3	34
100	Reduced light-induced degradation in a-Si:H: The role of network nanostructure. , 2011, , .		0
101	Epitaxial crystal silicon absorber layers and solar cells grown at 1.8 microns per minute. , 2011, , .		8
102	Junction transport in epitaxial film silicon heterojunction solar cells. , 2011, , .		3
103	Material quality requirements for efficient epitaxial film silicon solar cells. Applied Physics Letters, 2010, 96, 073502.	3.3	43
104	Mechanisms controlling the phase and dislocation density in epitaxial silicon films grown from silane below 800 A°C. Applied Physics Letters, 2010, 96, .	3.3	23
105	Physics and chemistry of hot-wire chemical vapor deposition from silane: Measuring and modeling the silicon epitaxy deposition rate. Journal of Applied Physics, 2010, 107, 054906.	2.5	12
106	Silicon quantum dot optical properties and synthesis: Implications for photovoltaic devices. , 2010, , .		0
107	Staebler-Wronski defects: Creation efficiency, stability, and effect on a-Si:H solar cell degradation. , 2010, , .		7
108	Photovoltaic-quality silicon epitaxy by hot-wire CVD at glasscompatible temperatures. , 2009, , .		0

#	Article	IF	CITATIONS
109	Epitaxial film silicon solar cells fabricated by hot wire chemical vapor deposition below 750°C. , 2009, , .		0
110	Phase evolution in nanocrystalline silicon films: Hydrogen dilution and the cone kinetics model. Philosophical Magazine, 2009, 89, 2461-2468.	1.6	1
111	Efficient black silicon solar cell with a density-graded nanoporous surface: Optical properties, performance limitations, and design rules. Applied Physics Letters, 2009, 95, .	3.3	286
112	Nanostructured black silicon and the optical reflectance of graded-density surfaces. Applied Physics Letters, 2009, 94, .	3.3	280
113	Cone Kinetics Model: Insights into the Morphologies of Mixed-phase Silicon Film Growth. Materials Research Society Symposia Proceedings, 2008, 1066, 1.	0.1	0
114	Quality and Growth Rate of Hot-wire Chemical Vapor Deposition Epitaxial Si Layers. Materials Research Society Symposia Proceedings, 2008, 1066, 1.	0.1	1
115	Metastable Defects in Light Soaked Amorphous Silicon at 77 K. Materials Research Society Symposia Proceedings, 2008, 1066, 1.	0.1	1
116	A new real-time quantum efficiency measurement system. Conference Record of the IEEE Photovoltaic Specialists Conference, 2008, , .	0.0	18
117	Cone kinetics model for two-phase film silicon deposition. Applied Physics Letters, 2008, 92, 093114.	3.3	15
118	Comparative Study of Solid-Phase Crystallization of Amorphous Silicon Deposited by Hot-wire CVD, Plasma-Enhanced CVD, and Electron-Beam Evaporation. Materials Research Society Symposia Proceedings, 2007, 989, 4.	0.1	6
119	ESR Study of Crystallization of Hydrogenated Amorphous Silicon Thin Films. Materials Research Society Symposia Proceedings, 2007, 989, 13.	0.1	0
120	Metastable Defects in Tritiated Amorphous Silicon. Materials Research Society Symposia Proceedings, 2007, 989, 4.	0.1	0
121	Significant improvement in silicon chemical vapor deposition epitaxy above the surface dehydrogenation temperature. Journal of Applied Physics, 2006, 100, 093520.	2.5	29
122	Physics of Solid-Phase Epitaxy of Hydrogenated Amorphous Silicon for Thin Film Si Photovoltaics. Materials Research Society Symposia Proceedings, 2006, 910, 5.	0.1	2
123	Combinatorial Studies of Switching and Solid-Phase Crystallization in Amorphous Silicon. Materials Research Society Symposia Proceedings, 2005, 894, 1.	0.1	0
124	Solid phase crystallization of hot-wire CVD amorphous silicon films. Materials Research Society Symposia Proceedings, 2005, 862, 1051.	0.1	12
125	Real Time Monitoring of the Crystallization of Hydrogenated Amorphous Silicon. Materials Research Society Symposia Proceedings, 2005, 862, 1611.	0.1	8
126	Increase of temperature and crystallinity during electrical switching in microcrystalline silicon. Materials Research Society Symposia Proceedings, 2004, 808, 185.	0.1	0

#	Article	IF	CITATIONS
127	Area-Dependent Switching in Thin Film-Silicon Devices. Materials Research Society Symposia Proceedings, 2003, 762, 1831.	0.1	2